Available online at www.sciencedirect.com
SCIENCE DIRECT®
Biomaterials 24 (2003) 3173–3181
Biomaterials
www.elsevier.com/locate/biomaterials

Characterisation and quantification of angiogenesis in β-tricalcium phosphate implants by immunohistochemistry and transmission electron microscopy

S. Henno, J.C. Lambotte, D. Glez, M. Guigand, G. Lancien, G. Cathelineau*

Équipe de Biomatériaux en Site Osseux, UMR CNRS 6511, Université de Rennes 1, 2 place Pasteur, 35000 Rennes, France

Received 17 July 2002; accepted 9 March 2003

Abstract

The aim of this study is the histological characterisation of angiogenesis in a macroporous biomaterial with quantification techniques used in oncology. Porous tricalcium phosphate implants were seated in the tibias of 12 rabbits. This work allows (1) morphological study with photonic microscopy, transmission electron microscopic and immunohistochemistry labelling for (2) quantification of vascularisation using anti-CD31 monoclonal antibody (3) quantification of proliferation using anti-PCNA polyclonal antibody (4) study of two angiogenic growth factors: VEGF and FGF-2.

Quantification of angiogenesis revealed an outbreak kinetic with early vascular growth in first several days and a second growth phase after 4 weeks. This study reveals in macropores many isolated cells without adjacent vascular lumen, with endothelial phenotype. Expression of angiogenic growth factors reveals that all endothelial cells were VEGF-negative throughout the test period. FGF-2 expression by endothelial cells began 2 weeks post-implantation. Osteoblasts strongly expressed two markers throughout the test period.

Furthermore, the procedure described here can be used to compare angiogenesis in different biomaterials or in the same biomaterial with the influence of macroporosities.

Keywords: Angiogenesis; Immunohistochemistry; TEM; Quantification; Tricalcium phosphate

1. Introduction

Vascularisation is essential to development, increase and functioning of all tissue. This process, particularly important in tissue repair, represents an essential preliminary condition in osseous reconstruction. Tissue injuries cause an inflammatory response whose intensity depends on numerous parameters, especially the causative agent and the tissue involved. The implantation of macroporous resorbable bone substitute biomaterials also causes those lesions, and the nature of the local tissue reaction induced determines the degree of tolerance [1–3]. Vascular involvement occurs at every stage of biomaterial/tissue interactions. Osteoconduction, and thus biomaterial substitution, depends on the quality of the colonisation. Angiogenesis is an essential step in the colonisation of macroporous biomaterials and during osteointegration. Capillaries bring osteoprogenitor cells and the nutriments that are required for their growth. They transport especially numerous angiogenic growth factors.

Few researchers have specifically studied angiogenesis in osteo-implants [4–10]. Neovascularisation in macroporous biomaterials implanted in osseous tissue developed from the medullary and periosteal vascular network in a centripetal direction [4]. Macroporous biomaterial consists of a framework in microvessel development. Vascular increase necessarily preceded osseous elaboration [9]. If impact of growth factors on vascularisation is now well known, their rules in capillaries development of macropores is unclear. King et al. [7] showed the interest of VEGF in endothelial cell growth in polymer contact.

The aim of this study is to highlight the mechanisms of vascular development in biomaterial macropores. We studied the blood vessels that colonised a macroporous

*Corresponding author. Tel.: +33-2-23-23-43-61; fax: +33-2-23-23-43-97.
E-mail address: guy.cathelineau@univ-rennes1.fr (G. Cathelineau).

0142-9612/03/$ - see front matter © 2003 Elsevier Science Ltd. All rights reserved.
doi:10.1016/S0142-9612(03)00149-2

ceramic biomaterial, tricalcium phosphate, implanted in rabbit tibias by adapting analytic methods used in oncology [11–15]. Vascularisation developed in the macropores of the biomaterial was studied and quantified with morphological techniques using histology on paraffin-embedded tissue and transmission electron microscopic (TEM). The proliferation and expression of angiogenic substances was then evaluated at the molecular level using immunohistochemical techniques.

2. Materials and methods

2.1. Animals

Twelve adult male New Zealand rabbits of the same age were distributed into four identical groups corresponding to four implantation periods (D15, D30, D45 and D60). We chose short periods because angiogenesis begins as soon as the biomaterial is implanted. The animals were kept in individual cages with appropriate temperature, ventilation, and hygrometric conditions in compliance with laboratory animal welfare regulations.

2.2. Biomaterial

A porous pure synthetic resorbable ceramic composed of β-tricalcium phosphate (TCP) (Calciresorb, Ceraver Osteal®) with a macroporosity of 45% was used. The implants were 20 mm in length and 6 mm in diameter. The macropores were 100–400 μm in diameter.

2.3. Biomaterial implantation

The biomaterial was implanted using the technique described by Lambotte et al. [16]. The rabbits were anaesthetised with intramuscularly injected Ketalar®. The lateral surfaces of the right and left knees were shaved. Local intradermal and subcutaneous anaesthesia was accomplished using Xylocaine®. Lateral, longitudinal incisions were made in the metaphyseal zone. A 6-mm diameter bit was used to bore the implantation sites. The implants were inserted and securely anchored.

2.4. Bone sample removal

The rabbits were euthanised on days 15, 30, 45, and 60. The tibias were dissected and removed. Transverse sections 1 cm above and below the implant sites were performed. Longitudinal sections through the centres of the implants were also cut.

2.5. Immunohistochemistry

The two bone samples from the right tibias were fixed in 10% formaldehyde for 24 h and then demineralised in 5% nitric acid for 6 h. They were rinsed, refixed in formaldehyde for 24 h, and demineralised again for 4–6 h. They were then embedded in paraffin and cut into 4–5-μm-thick sections. One section was stained with hematoxylin–eosin–safranine (HES). Four sections were placed on silanised slides for the immunohistochemical techniques. After removing the paraffin, the sections were rehydrated, placed in a citrate solution (pH 6), and heated in a microwave oven for three 5-min treatments. Endogenous peroxidases were inhibited with hydrogen peroxide, and biotin was inhibited using an endogenous avidin/biotin blocking kit (ZYMED®). Immunodetection of antigens was performed using the streptavidine/biotin/peroxidase technique (LSAB kit, DAKO®). All the primary antibodies were incubated for 30 min at room temperature: (i) anti-CD31 (JC/70A monoclonal antibody, DAKO®) diluted 1/20, (ii) anti-PCNA (5A10 monoclonal antibody, IMMUNOTECH®) diluted 1/250, (iii) anti-VEGF (monoclonal antibody, SANTA CRUZ®) diluted 1/200, and (iv) anti-FGF-2 (polyclonal antibody, SANTA CRUZ®) diluted 1/400.

After counterstaining with Mayer's haematoxylin, the sections were mounted in glycergel (DAKO®). Positive (a muscle sample rich in blood vessels for CD31 and FGF-2 and a liver sample for VEGF) and negative controls (primary antibody replaced by buffer) were included with each reaction.

2.6. Transmission electron microscopy

Sections from the left tibias were placed on binocular magnifying glass. One-mm-square blocks of biomaterial were removed from the biomaterial/bone interface and fixed in 2.5% glutaraldehyde for 10 h at 4°C. They were rinsed in 0.2 M cacodylate buffer and demineralised for 30 min in 5% nitric acid. The blocks were post-fixed in osmic acid for 1 h at 4°C, placed in agarose, and dehydrated in graded alcohol baths. The blocks were then embedded in epon/propylene oxide, which was left to polymerise for 12 h at room temperature. The embedded blocks were incubated for 48 h at 60°C. Thin and semi-thin (0.15 μm) sections were cut and stained with uranyl acetate for 30 min and lead citrate for 15 min.

2.7. Evaluation of angiogenesis

2.7.1. Morphological analysis

The HES-stained sections were examined using a light microscope. The uranyl acetate/lead citrate-stained sections were examined using a transmission electron microscope in order to localise endothelial cells.

2.7.2. Quantification of vascularisation

CD31 is a cell adhesion molecule that is strongly expressed by endothelial cells. The CD31-labelled and

HES-stained sections were examined using a microscope connected to a computer equipped with image analysis software (Histolab, MICROVISION®) that allowed semi-automatic measurements to be taken. To limit counting bias, we calculated densities and areas on complete implant sections. The counts of the total number of vessels and vascular sections were done on immunolabelled sections. A vessel was defined as any structure that was immunolabelled with the anti-CD31 antibody, whether or not a recognisable lumen could be seen. A vascular section was defined as a vessel with a recognisable lumen. HES-stained sections were used for the measurements of total vascular surface and average vascular perimeters and diameters.

2.7.3. Quantification of vascular proliferation

Given that endothelial cells proliferate slowly, we selected PCNA as a proliferation marker since it has a long half-life. While all proliferating cells express PCNA, we only counted endothelial cells. The total number of labelled endothelial cells with respect to the total number of endothelial cells was assessed at a magnification of 400. The entire biomaterial surface was examined on each section and the result was expressed as a percentage of labelled cells.

2.7.4. Evaluation of angiogenic factors

Expression of VEGF and FGF-2 by the various cell types was evaluated qualitatively as a function of sampling day.

3. Results

3.1. Morphological analysis

Progressive colonisation from the periphery to the centre of the macropores of the biomaterial could be seen on the HES-stained slides from D15 to D60. The TCP was gradually replaced by bone tissue over the same period. On D15, osteoformation and highly vascularised connective tissue could be seen in the most peripheral macropores (Fig. 1). The capillaries were small and surrounded by turgid endothelial cells. Osteoblasts formed a palisade-like border at the periphery of the macropores. On D30, the capillaries were larger in size (Fig. 2) and by D60, almost all the pores were colonised.

The TEM examination revealed that the morphology of the endothelial cells bordering the capillaries was normal and that their cytoplasm contained numerous organites (Fig. 3). Weibel–Pallade bodies were not observed. Isolated elongated cells were also observed in a collagen matrix devoid of vascular lumen (Fig. 4).

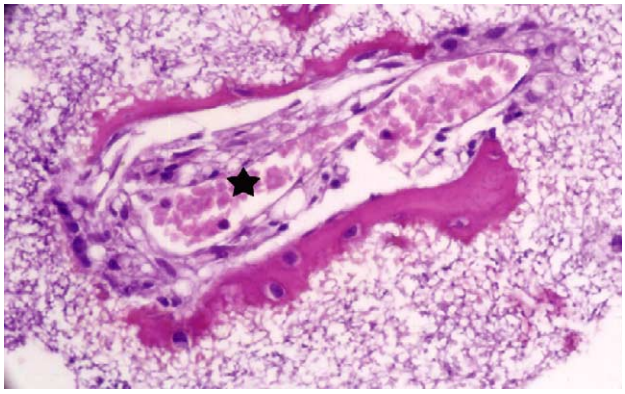

Fig. 1. Colonisation of a macropore on D30: large capillary at the centre of the pore (★), mineralised bone replacing the biomaterial along the border of a macropore (HES, ×400).

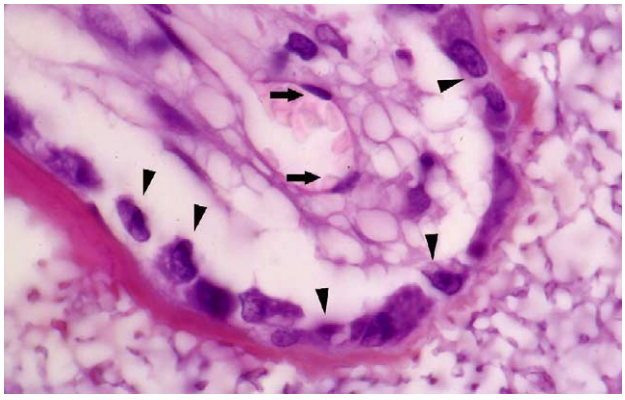

Fig. 2. Detail of a macropore on D60: endothelial cell nuclei (→), osteoblasts bordering a macropore (▼) (HES, ×1000).

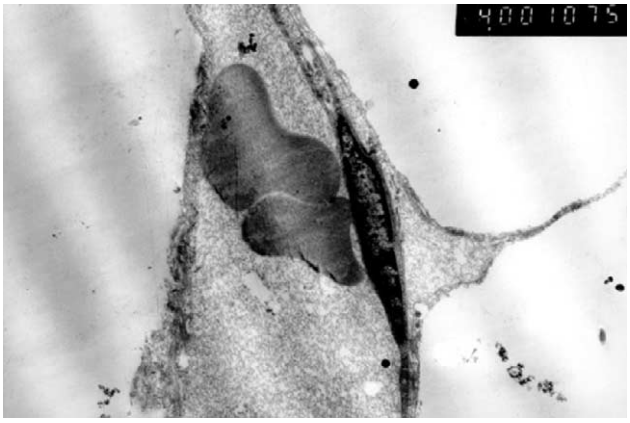

Fig. 3. Isolated endothelial cell on D15 in connective tissue with no identifiable vascular lumen (TEM, ×4000).

3.2. Quantification of vascularisation

The results are shown in Table 1. Vascularisation was quantified using CD31-labelled sections (Fig. 5). The biomaterial surface that was replaced by organic tissue

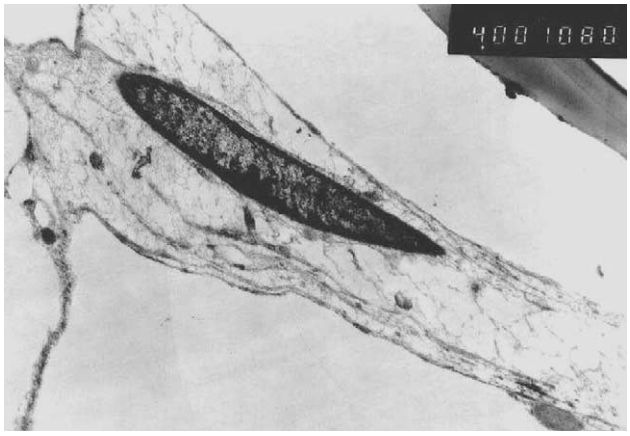

Fig. 4. Endothelial cell on D60 bordering a vessel containing erythrocytes (TEM, ×6700).

increased over time. It represented an average of 3.7% of the total surface on D15, and 38.5% on D60. Vessels made up 5.5% on average of the organic tissue colonising the macropores. Vascular density (D/A) decreased over time. Fewer vascular sections and vessels were seen at D30 than D15, but increased at D45 and D60 (Fig. 6). $C-D$, which corresponds to vascular structures devoid of lumen, decreased over time (averages: D15 = 17%; D30 = 12.8%; D45 = 5%; D60 = 2.8%). Average vascular diameters and perimeters had a similar progression and were greatest at D30 (Fig. 7).

3.3. Quantification of vascular proliferation

The results are shown in Table 1 and are based on nuclei labelling (Fig. 8). The overall average for the expression of proliferation markers was 7.8% (8% at D15, 8.7% at D30, 8% at D45, and 6.7% at D60).

3.4. Evaluation of angiogenesis factors

The endothelial cells did not express the VEGF marker, while intense, diffuse cytoplasmic labelling was seen in almost all the osteoblasts bordering the TCP macropores on all sampling days (Fig. 9).

The endothelial cells did not express FGF-2 marker on D15. On D30 and D60, labelling in the most peripheral macropores could be seen in a few cells (Fig. 10). The osteoblasts bordering the TCP macropores strongly expressed FGF-2 on all sampling days.

4. Discussion

We chose the rabbit model because it has been widely used in studies on osteo-integrated biomaterial implants [10,16–22]. Tricalcium phosphate ceramic, which is commonly used as a bone substitute, was implanted in

Table 1
Results of morphological analysis

No.	Duration of implantation (days)	Total implant surface (mm^2)	A = biomaterial surface colonised (mm^2)	B = total vascular surface (mm^2)	B/A (%)	C = total number of vessels	D = total number of vascular sections	$C-D$ (%)	D/A (sections/mm^2)	Average vascular diameter (μm)	Average vascular perimeter (μm)	PCNA (%)
1	15	23.4	0.88	0.052	5.9	215	187	13	212	15.5	63.9	9.1
2	15	22.9	0.87	0.062	8.7	267	217	18.7	249	17.6	72.7	9.7
3	15	23	0.86	0.038	5.0	201	162	19.4	188	15	61.1	5.2
4	30	19	1.45	0.090	6.2	129	109	15.5	75	27.9	108	13
5	30	22.8	1.21	0.089	7.3	129	111	13.9	92	51.3	180.7	5.7
6	30	23.1	1.04	0.062	5.9	132	120	9	115	26.2	132	7.3
7	45	27.5	2.31	0.088	3.8	250	233	6.8	101	18.9	74	9.7
8	45	28.2	4.47	0.093	4.3	399	374	5.2	83	20.9	84.6	6
9	45	26.9	3.69	0.090	2.4	296	287	3	78	23.2	97	8.2
10	60	22.3	8.63	0.60	6.9	617	612	0.8	71	30.0	113	10
11	60	23.8	8.69	0.47	4.9	607	587	3.3	67	28.3	111.4	4.3
12	60	20.4	8.26	0.43	5.7	557	533	4.4	64	26	107	5.7

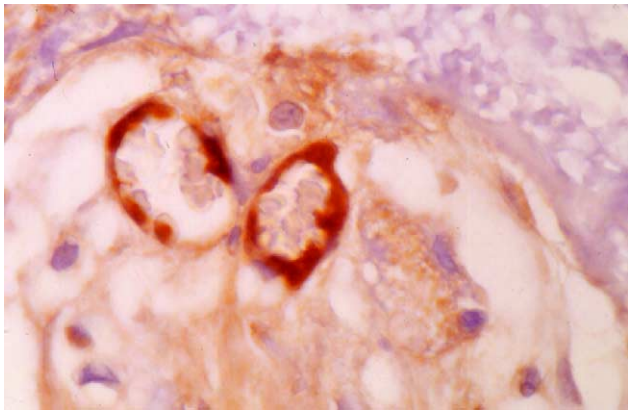

Fig. 5. CD31-immunolabelled endothelial cells bordering two vascular sections (× 1000).

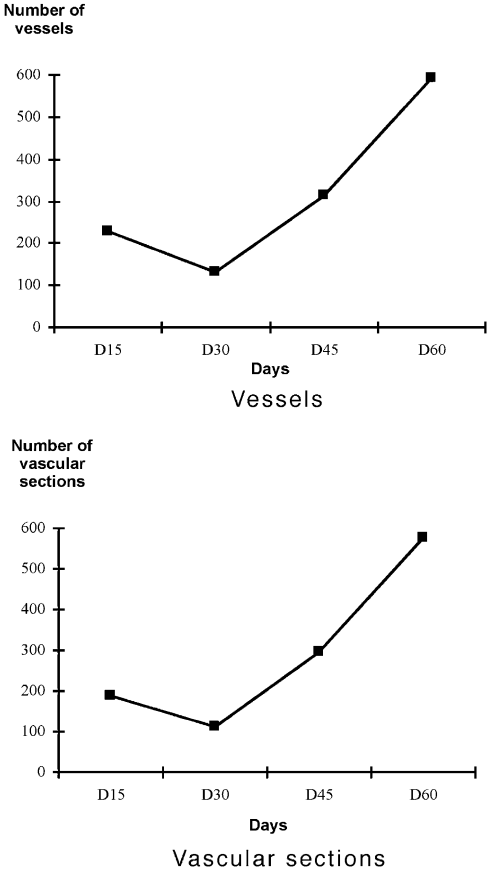

Fig. 6. Change in the average number of vessels and vascular sections.

both tibias of the rabbits to ensure a sufficient amount of material for both the immunohistochemical and electron microscopic studies. This bioactive, biocompatible, osteoconductive biomaterial has already been characterised in detail.

4.1. Morphological evaluation

TCP implants that we used present a size between 100 and 400 μm. Their size allows the colonisation by

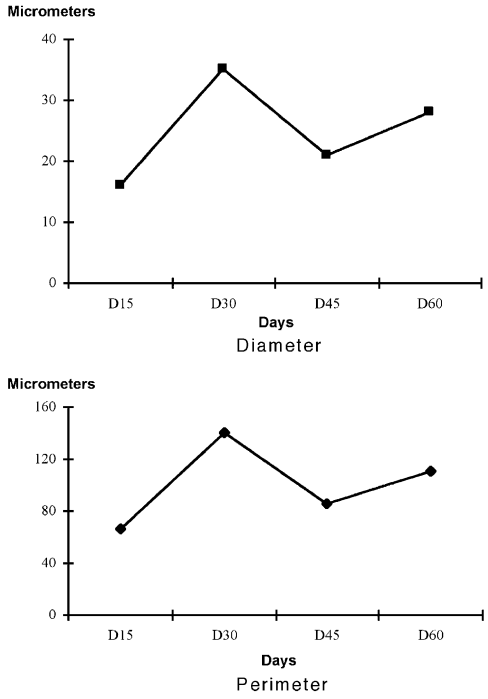

Fig. 7. Change in average vascular diameters and perimeters.

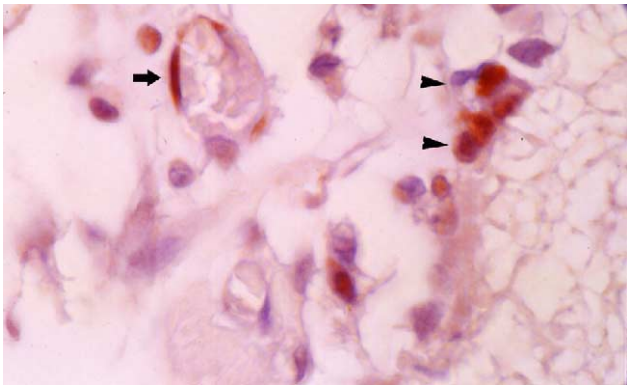

Fig. 8. PCNA-immunolabelled endothelial cell (→) and osteoblast (▼) nuclei (× 1000).

neovessels. The interconnection of these pores leads to the emergence of a vascular anastomotic network. The biomaterial is gradually degraded with an accompanying enlargement of the macropores [23], which contain numerous vascular sections [5]. Osteoformation can be seen within 2 weeks of implantation [24], and practically all the pores of the biomaterial are colonised within 2 months [25]. The morphological results indicating a progressive replacement of TCP by bone tissue were in agreement with those reported in the literature.

4.2. Vascularisation quantification

In oncology, high microvessel density is frequently associated with a poor prognosis. The techniques used

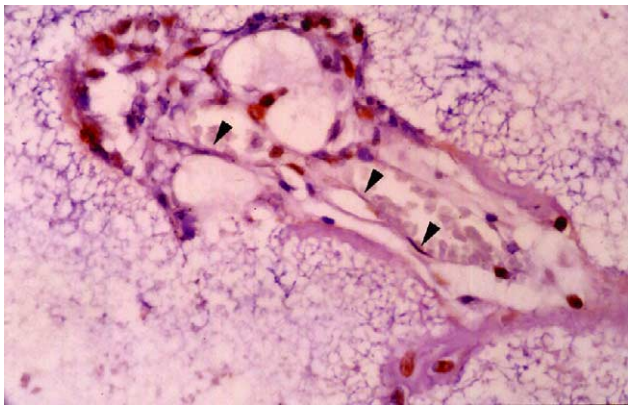

Fig. 9. Unlabelled (VEGF) endothelial cells (▼), VEGF-immunolabelled osteoblasts bordering a pore (× 400).

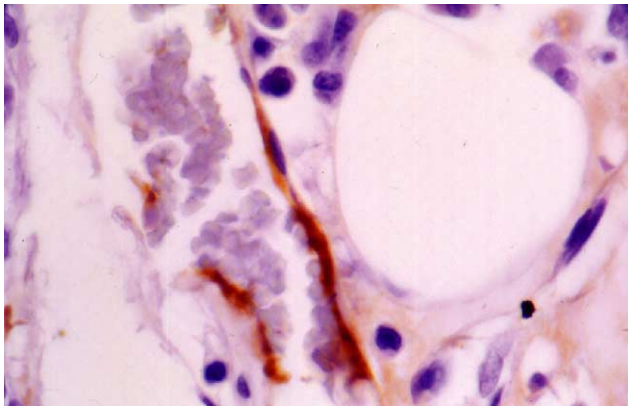

Fig. 10. Detail of the FGF-2-immunolabelled cytoplasm of an endothelial cell on D45 (× 1000).

in oncology have never been tested with inflammatory pathologies, especially for evaluating biomaterial contact angiogenesis. In 1972, before the advent of immunohistochemical techniques, Brem et al. [26] emphasised the limits of solely using morphological examinations to count the number of vessels. This was confirmed by our study since a larger number of vessels were detected on CD31-labelled sections than on HES-stained sections. This is even more evident during the early stages of angiogenesis.

The total vascular surface represented a small percentage (2.4–8.7%) of the tissue colonising the pores. The percentage remained constant throughout the experimental period, indicating that vessel growth matched that of the other cells colonising the pores. The number of vascular sections was lowest at D30, but the average vascular diameter and perimeter increased substantially, resulting in larger capillaries in the pores. The decrease in average vascular diameter and perimeter at D45 combined with a large increase in the number of vascular sections indicated that a second phase of vascular outgrowth from existing capillaries occurred after D30 and continued until D60 (insertion of Fig. 11).

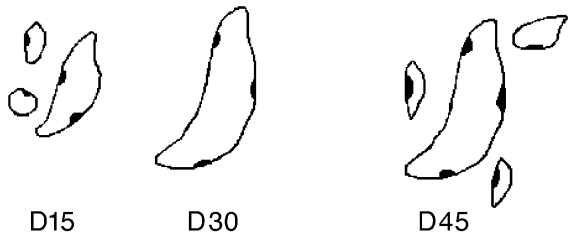

Fig. 11. Evolution of vascular outgrowth.

The fusion of capillary sprouts to form vessels with larger lumen during angiogenesis has been described previously [27,28]. However, our results must be interpreted with care because of the small number of samples.

There is a close relationship between the intimacy of bone apposition and the adjacent vascular surface during growth [29]. By analogy, an identical mechanism may be a work in macroporous biomaterials. The quality of vascularisation in terms of density and surface area would thus be a good indicator of osteointegration. Other results provide additional support for this hypothesis. For example, Ohgushi et al. [30] have reported that cell reactions in the pores of macroporous ceramics differ depending on the nature of the ceramic. A recent histological study looked at cell reactions around two biomaterials (aluminium calcium phosphate and hydroxyapatite) implanted subcutaneously and intraperitoneally in rats [31]. The authors observed a difference in vascular density between the two biomaterials.

4.3. Vascular development in macropores

New blood vessels in implant macropores grow from the vessels at the biomaterial interface. It has also been shown that apparently isolated cells migrate into connective tissue [27]. These microvessels, which are devoid of lumen, are not always easy to identify on histological sections, which is why immunohistochemical techniques are so important. Immunolabelling with CD31 reveals with accuracy the development of the vascular network. This labelling identifies not only the vessels with a lumen, which are visible on standard stainings, but also some isolated cellular elements, particularly in early stages (D15 and D30). The isolated cells with an endothelial-like morphology expressed CD-31 and FGF-2, but not VEGF, which is the immunohistochemical phenotype of endothelial cells. These isolated progenitor cells are also revealed in our TEM observations. Most likely these isolated cells migrate from adjacent newly formed vessels in order to lead to the formation of other vessels. Thus, it is necessary to

modify their adhesion ability, may be in GAP junction. Their role in the control of angiogenesis has been demonstrated [32].

Very few ultrastructural studies of endothelial cells involved in angiogenesis have been published. However, Mompeo et al. [33] have reported the presence of isolated, migrating endothelial cells in the tissues of diabetic patients. The morphology of the endothelial cells was modified during this pathological angiogenesis process. We observed no apparent morphological modifications of vessels and endothelial cells by TEM from D15 to D60. Care must be used in interpreting this result given the small number of samples examined and the changes induced by the demineralisation. Furthermore, a morphological study, even at the ultrastructural level, is insufficient to identify endothelial cells with certainty [34]. As was the case with the histological sections, we observed cells by TEM that had the morphological properties of endothelial cells. However, they were limited to the collagen matrix and did not border the vascular lumen. These cells corresponded to the migrating cells in the connective tissue.

Some authors have suggested that osteoblasts arise from the differentiation of vascular cells [35]. In a recent study on pulp vascularisation, Carlile et al. [36] showed that pericytes migrate from vessels and modify their morphology to resemble fibroblasts. An analysis of the literature and our results showed that isolated, mesenchymal cells with a vascular phenotype can migrate from vessels and, depending on various stimuli and the cell microenvironment, can differentiate into osteoprogenitor or endothelial cells.

4.4. Vascular proliferation

Very few studies in the fields of inflammatory pathologies and biomaterial implantation have looked at proliferation markers. Hagerty et al. [37] used proliferation markers to evaluate cell proliferation around a biomaterial implanted in rats. On our sections, the labelling was clearly discernable and the background (non-specific labelling) was insignificant to non-existent. PCNA, however, is not specific to a single cell type so all proliferating cells are labelled. While proliferating osteoblasts were easily identifiable, and were thus not included in the cells counts, fibroblasts and endothelial cells were more difficult to differentiate, especially when there was no visible vascular lumen. The cell counts showed that the percentage of proliferating endothelial cells labelled with anti-PCNA remained relatively constant over time and never exceeded an average of 9%. This can be used as a reference for comparing the results obtained with other biomaterials in order to determine which architectural and chemical properties influence vascular proliferation. Angiogenesis markers have already been evaluated using tissues from numerous human tumour and non-tumour pathologies.

4.5. Angiogenic growth factor

VEGF is considered the driving force behind the angiogenesis process [38]. It acts in conjunction with FGF-2 in the proliferation and migration phases of endothelial cells [39]. Numerous cell types express VEGF and FGF-2 [40–42], including osteoblasts and certain inflammatory cells. Studies using FGF-2 must be conducted with care since only endothelial cells (positive and negative) must be counted. The stimulation of endothelial cells by angiogenic factors is an extremely complex phenomenon. Certain authors consider FGF-2 the main angiogenic factor in capillaries [43]. The fact that the endothelial cells were not labelled at D15 suggests that the expression of FGF-2 was delayed. We observed strong neovascularisation between D15 and D30. This strong growth may have been due to FGF-2, which comes into play mainly 15 days post-implantation. Osteoblasts express constant, high levels of VGEF, which are FGF-2 and dose-dependent [44]. In our study, the endothelial cells did not express FGF-2 during the first 15 days post-implantation, which suggests that osteoblasts are the main source of angiogenic factors in the early phase of angiogenesis. Many growth factors demonstrate pro-angiogenic activity, and a number of reports have indicated that it would be useful to use them in conjunction with biomaterials to improve osteointegration. TGF-β1 [45] and IGF1 [46], which are known pro-angiogenic factors, have both been shown to enhance bone growth in TCP implants. However, Bland et al. [47] have reported that FGF-2 has no positive impact on fracture repair in rabbits, and so further testing is required.

5. Conclusion

The understanding of angiogenesis mechanisms in macropores needs a better characterisation of osteointegration in macroporous biomaterials.

As far as this biomaterial, frequently used in orthopaedic surgery, is concerned, this study makes it possible to define the mechanisms of capillary development in macropores. Quantification of angiogenesis revealed an outbreak kinetic with early vascular growth in first several days and a second growth phase after 4 weeks with fusion of vascular buds. Isolated cells with endothelial phenotype have been highlighted. The migration mechanisms of these cells and their role in angiogenesis and osteogenesis still have to be defined more accurately. Lastly, the role of angiogenic growth factors in the colonisation of macroporosities has been demonstrated.

In this, a range of morphological and molecular evaluations that combine histological, immunohistochemical, and electron microscopic techniques make it possible not only to better characterise angiogenesis in resorbable macroporous biomaterial bone substitutes. These techniques also make it possible to evaluate the effect of porosity on angiogenesis but also to compare biomaterials and evaluate the impact of angiogenesis on osteointegration. Lastly, angiogenic growth factors and their impact on the speed and quality of bone substitution must be studied.

Acknowledgements

The authors would like to thank CERAVER OSTEAL® for providing the biomaterial samples, Pascale Bellaud and Florence Jouan for technical assistance, and Gene Bourgeau and Céline Allaire for editorial assistance.

References

[1] Remes A, Williams DF. Immune response in biocompatibility. Biomaterials 1992;13:731–43.
[2] Tang L, Eaton JW. Inflammatory responses to biomaterials. Am J Clin Pathol 1995;103:466–71.
[3] Williams DF. Biocompatibility: performance in the surgical reconstruction of man. Int Sci Rev 1990;15:20–3.
[4] Bush D, England B, Tucci M, Cason Z, Lemos L, Benghuzzi H. The effect of TCPL devices on tissue–implant interface analysis using adult sheep as a model. Biomed Sci Instrum 1995;31:147–52.
[5] Chang CS, Su CY, Lin TC. Scanning electron microscopy observation of vascularization around hydroxyapatite using vascular corrosion casts. J Biomed Mater Res 1999;48:411–6.
[6] Collier JH, Camp JP, Hudson TW, Schmidt CE. Synthesis and characterization of polypyrrole-hyaluronic acid composite biomaterials for tissue engineering applications. J Biomed Mater Res 2000;50:574–84.
[7] King TW, Patrick Jr CW. Development and in vitro characterization of vascular endothelial growth factor (VEGF)-loaded poly(DL-lactic-*co*-glycolic acid)/poly(ethylene glycol) microspheres using a solid encapsulation/single emulsion/solvent extraction technique. J Biomed Mater Res 2000;51:383–90.
[8] Rubin PA, Nicaeus TE, Warner MA, Remulla HD. Effect of sucralfate and basic fibroblast growth factor on fibrovascular ingrowth into hydroxyapatite and porous polyethylene alloplastic implants using a novel rabbit model. Ophthalmol Plast Reconstr Surg 1997;13:8–17.
[9] Schmid J, Wallkamm B, Hammerle CH, Gogolewski S, Lang NP. The significance of angiogenesis in guided bone regeneration. A case report of a rabbit experiment. Clin Oral Implants Res 1997;8:244–8.
[10] Winet H, Hollinger JO, Stevanovic M. Incorporation of polylactide–polyglycolide in a cortical defect: neoangiogenesis and blood supply in a bone chamber. J Orthop Res 1995;13:679–89.
[11] Barbareschi M, Gasparini G, Morelli L, Forti S, Dalla Palma P. Novel methods for the determination of the angiogenic activity of human tumors. Breast Cancer Res Treat 1995;36:181–92.
[12] Fox SB, Leek RD, Weekes MP, Whitehouse RM, Gatter KC, Harris AL. Quantitation and prognostic value of breast cancer angiogenesis: comparison of microvessel density, Chalkley count, and computer image analysis. J Pathol 1995;177:275–83.
[13] Hansen S, Grabau DA, Rose C, Bak M, Sorensen FB. Angiogenesis in breast cancer: a comparative study of the observer variability of methods for determining microvessel density. Lab Invest 1998;78:1563–73.
[14] Kato T, Kimura T, Ishii N, Fujii A, Yamamoto K, Kameoka S, Nishikawa T, Kasajima T. The methodology of quantitation of microvessel density and prognostic value of neovascularization associated with long-term survival in Japanese patients with breast cancer. Breast Cancer Res Treat 1999;53:19–31.
[15] Weidner N. Current pathologic methods for measuring intratumoral microvessel density within breast carcinoma and other solid tumors. Breast Cancer Res Treat 1995;36:169–80.
[16] Lambotte JC, Thomazeau H, Cathelineau G, Lancien G, Minet J, Langlais F. Tricalcium phosphate, an antibiotic carrier: a study focused on experimental osteomyelitis in rabbits. Chirurgie 1998;123:572–9.
[17] Daculsi G, Legeros JP. Three-dimensional defects in hydroxyapatite of biological interest. J Biomed Mater Res 1996;31:495–501.
[18] Richard M, Aguado E, Cottrel M, Daculsi G. Ultrastructural and electron diffraction of the bone–ceramic interfacial zone in coral and biphasic CaP implants. Calcif Tissue Int 1998;62:437–42.
[19] Schroeder JA, Brown MK. Biocompatibility and degradation of collagen bone anchors in a rabbit model. J Biomed Mater Res 1999;48:309–14.
[20] Trecant M, Delecrin J, Royer J, Goyenvalle E, Daculsi G. Mechanical changes in macroporous calcium phosphate ceramics after implantation in bone. Clin Mater 1994;15:233–40.
[21] Vogely HC, Oosterbos CJ, Puts EW, Nijhof MW, Nikkels PG, Fleer A, Tonino AJ, Dhert WJ, Verbout AJ. Effects of hydrosyapatite coating on Ti-6A1-4V implant-site infection in a rabbit tibial model. J Orthop Res 2000;18:485–93.
[22] Winet H, Hollinger JO. Incorporation of polylactide–polyglycolide in a cortical defect: neoosteogenesis in a bone chamber. J Biomed Mater Res 1993;27:667–76.
[23] Shimazaki K, Mooney V. Comparative study of porous hydroxyapatite and tricalcium phosphate as bone substitute. J Orthop Res 1985;3:301–10.
[24] Gunther KP, Scharf HP, Pesch HJ, Puhl W. Integration properties of bone substitute materials. Experimental studies on animals. Orthopade 1998;27:105–17.
[25] Daculsi G, Passuti N, Martin S. Etude comparative de céramiques bioactives en phosphate de calcium après implantation en site osseux spongieux chez le chien. Rev Chir Orthop 1989;75:65–71.
[26] Brem S, Cotran R, Folkman J. Tumor angiogenesis: a quantitative method for histologic grading. J Natl Cancer Inst 1972;48:347–56.
[27] Alberts B, Bray D, Lewis J, Raff M, Roberts K, Watson JD. Differentiated cells and the maintenance of tissues. Mol Biol Cell 1994;5:573.
[28] Vernon RB, Sage HE. Between molecules and morphology: extracellular matrix and creation of vascular form. Am J Pathol 1995;147:873–83.
[29] Marotti G, Zallone AZ. Changes in the vascular network during the formation of Haversian systems. Acta Anat 1980;106:84–100.
[30] Ohgushi H, Okumura M, Yoshikawa T, Inoue K, Senpuku N, Tamai S, Shors EC. Bone formation process in porous calcium carbonate and hydroxyapatite. J Biomed Mater Res 1992;26:885–95.
[31] Butler K, Benghuzzi H, Puckett A. Cytological evaluation of the tissue–implant reaction associated with S/C and I/P implantation of ALCAP and HA bioceramics in vivo. Pathol Res Pract 2001;197:29–39.

[32] Dejana E, Spagnuolo R, Bazzoni G. Interendothelial junctions and their role in the control of angiogenesis, vascular permeability and leukocyte transmigration. Thromb Haemost 2001;86:308–15.
[33] Mompeo B, Ortega F. Immunohistochemical and ultrastructural study of microvessels in diabetic veins. Ultrastruct Pathol 1999;23:25–31.
[34] Craig LE, Spelman JP, Strandberg JD, Zink MC. Endothelial cells from diverse tissues exhibit differences in growth and morphology. Microvasc Res 1998;55:65–76.
[35] Decker B, Bartels H, Decker S. Relationships between endothelial cells, pericytes, and osteoblasts during bone formation in the sheep femur following implantation of tricalciumphosphate-ceramic. Anat Rec 1995;242:310–20.
[36] Carlile MJ, Sturrock MG, Chisholm DM, Ogden GR, Schor AM. The presence of pericytes and transitional cells in the vasculature of the human dental pulp: an ultrastructural study. Histochem J 2000;32:239–45.
[37] Hagerty RD, Salzmann DL, Kleinert LB, Williams SK. Cellular proliferation and macrophage populations associated with implanted expanded polytetrafluoroethylene and polyethyleneterephthalate. J Biomed Mater Res 2000;49:489–97.
[38] Amoroso A, Del Porto F, Di Monaco C, Manfredini P, Afeltra A. Vascular endothelial growth factor: a key mediator of neoangiogenesis. A review. Eur Rev Med Pharmacol Sci 1997;1:17–25.
[39] Ortega N, Jonca F, Vincent S, Favard C, Ruchoux MM, Plouet J. Systemic activation of the vascular endothelial growth factor receptor KDR/flk-1 selectively triggers endothelial cells with an angiogenic phenotype. Am J Pathol 1997;151:1215–24.
[40] Folkman J, Shing Y. Angiogenesis. J Biol Chem 1992;267:10931–4.
[41] Rifkin DB, Moscatelli D. Recent developments in the cell biology of basic fibroblast growth factor. J Cell Biol 1989;109:1–6.
[42] Thomas KA. Vascular endothelial growth factor, a potent and selective angiogenic agent. J Biol Chem 1996;271:603–6.
[43] D'Amore PA, Smith SR. Growth factor effects on cells of the vascular wall: a survey. Growth Factors 1993;8:61–75.
[44] Saadeh PB, Mehrara BJ, Steinbrech DS, Spector JA, Greenwald JA, Chin GS, Ueno H, Gittes GK, Longaker MT. Mechanisms of fibroblast growth factor-2 modulation of vascular endothelial growth factor expression by osteoblastic cells. Endocrinology 2000;141:2075–83.
[45] Lin M, Overgaard S, Glerup H, Soballe K, Bunger C. Transforming growth factor-beta1 adsorbed to tricalciumphosphate coated implants increases peri-implant bone remodeling. Biomaterials 2001;22:189–93.
[46] Laffargue P, Fialdes P, Frayssinet P, Rtaimate M, Hildebrand HF, Marchandise X. Adsorption and release of insulin-like growth factor-I on porous tricalcium phosphate implant. J Biomed Mater Res 2000;49:415–21.
[47] Bland YS, Critchlow MA, Ashhurst DE. Exogenous fibroblast growth factors-1 and -2 do not accelerate fracture healing in the rabbit. Acta Orthop Scand 1995;66:543–8.